

# A Broadband Beam-Steered Fiber Mm-Wave Link with High Energy-Spectral-Spatial Efficiency for 5G Coverage

Z. Cao, X. Zhao, Y. Jiao, X. Deng, N. Tessema, O. Raz, and A. M. J. Koonen

COBRA Research Institute, Eindhoven University of Technology, PO Box 513, 5600MB Eindhoven, The Netherlands

Author e-mail address: [z.cao@tue.nl](mailto:z.cao@tue.nl)

**Abstract:** Utilizing an integrated optical-tunable-delay-line, reversely-modulated single sideband modulation, and Nyquist subcarrier modulation, we demonstrate an 8 Gbps mm-wave beam steered link with a spatial-spectral efficiency of 16 bits/s/Hz.

**OCIS codes:** (060.5625) Radio frequency photonics; (070.1170) Analog optical signal processing

## 1. Introduction

New architectures for the next generation mobile communications (5G) are driven by a lot of factors, but it is widely recognized that operators need more capacity at a lower total cost of ownership. These small cell extensions allow carriers to add capacity or coverage in a more targeted manner. Usually, mobile backhails are built on fiber links. However, at fiber link ends, a low cost and flexible solution is demanded for hard-to-wire locations. These days the 28/38 GHz mm-wave bands are currently under extensive evaluation for 5G and licenses for these bands could be released soon [1]. The radio over fiber (RoF) technique operating at mm-wave band is a good option to extend the fiber link coverage. The optical-electrical-optical conversion loss and the electrical bottlenecks are two major issues. High modulation efficiency and electrical-device-less configurations are highly desired. Radio beam steering (RBS) based on optical true time delay (OTTD) schemes can provide inherent broadband narrow beams (thus high power / spatial-spectral efficiency) and wireless spatial switching, which can greatly benefit the mobile backhaul. Combined with RoF networks, the cost can be reduced by sharing the common optical transmitters. Complicated configurations and bulk sizes of the traditional OTTD-RBS schemes limit their applications [2]. To reduce the maintenance/building cost, a remotely-controllable photonics integrated beamformer is the key for large-scale applications [3-6]. Recently, we designed and characterized a remotely tuning integrated optical tunable delay line (OTDL) based on an arrayed waveguide grating feedback loop (AWG-loop), which allows a compact, fabrication tolerant and scalable solution [3]. An optical mm-wave beam steered link with 25 Mbps data rate is demonstrated based on the integrated AWG-loop. In this paper, we aim to boost the capacity while simplifying the whole system for the mobile backhaul applications. To reduce the optical transmitter complexity, a single reversely-modulated dual-electrode MZM without electrical mixers is used for high optical modulation efficiency and electrical-bottleneck-free operation. Since mobile backhails do not require a heavy multi-user access control, the single carrier half-cycled (HC) QAM-16 signal with low peak-to-average ratio (compared to OFDM) is employed for high modulation efficiency and high spectral efficiency of 4 bits/s/Hz. With these enabling techniques, a simplified RoF link with beam steering capability is demonstrated exceeding 16 bits/s/Hz (4 spatial channels  $\times$  4 bits/s/Hz) spatial-spectral efficiency with 14 dB channel isolation. To the best of our knowledge, this is the first demonstration of 8 Gbps data with 16 bits/s/Hz efficiency at mm-wave bands based on a remotely-controllable integrated OTDL.

## 2. Integrated wavelength-tunable AWG-loop delay networks

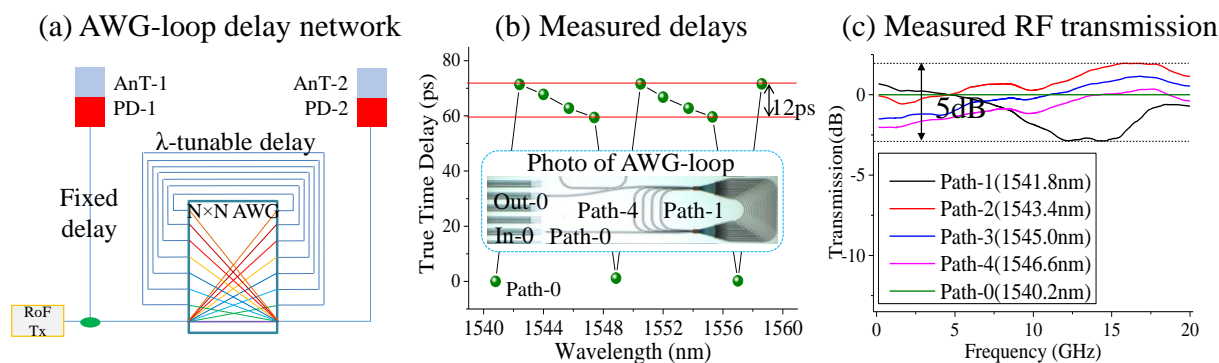


Fig. 1. The integrated wavelength-controllable AWG-loop delay networks and the corresponding measured delays

The operation principle of our optical millimeter wave (mm-wave) beam steering system is shown in Fig. 1(a). The optical mm-wave modulated with data is generated from a radio over fiber transmitter (RoF Tx). It is then split into two branches. One is fed to a photodiode (PD-1) cascaded with an antenna (AnT-1) with a fixed delay induced by the fiber. The other is fed to PD-2 followed by AnT-2 with a wavelength-tunable delay. As the central wavelength of the optical mm-wave signal is tuned, the delay difference between AnT-1 and AnT-2 is tuned, which results in the mm-wave beam steering. In our system, the wavelength-tunable delay is based on an integrated AWG-loop with its photo shown in Fig. 1(b). The core component of the AWG-loop is a spectral-cyclic 5-by-5 AWG. Its free spectral range (FSR) is 8 nm (1000 GHz). The channel spacing (CS) is 1.6 nm (200 GHz) and its -3-dB passband is 0.52 nm (65 GHz). The waveguides connect four pairs of inputs and outputs to form the feedback loops with different delays. One pair of input and output of the AWG (In-0, Out-0) is used as the input and output of the AWG-loop and is connected to two spot size convertors (SSCs). The footprint of the AWG-loop is  $2.6 \times 1.2 \text{ mm}^2$ . The maximum insertion loss of the AWG-loop is 6.5 dB without SSC coupling loss. The maximum delay (Path-4) is designed to be 12.5 ps for  $\pi$  phase shift at 40 GHz. The designed delays of Path-1 to Path-4 increase progressively with a range of 12.5 ps. A time domain correlation method is used for delay measurement. As shown in Fig. 1(b), the measured delays linearly increase from Path-1 to Path-4 with a delay range of 12 ps, which is a little smaller than the one we expected. The differences between the designed delays and the measured ones for Path-1 to Path-4 are -0.5, 0.1, -0.76 and 0 ps from 1540 to 1548 nm. The acceptable match between the designed delays and measured ones demonstrate a high design accuracy. As shown in Fig. 1(c), we measured the radio frequency (RF) transmission curve of the AWG-loop by an electrical vector network analyzer (VNA) with a measurement range from 130 MHz to 20 GHz. The Path-0 without feedback loop is used as a referenced path. The -3-dB bandwidth of the AWG is 65 GHz, which is much higher than the frequency range of the VNA. Therefore, the AWG filtering effect does not contribute significantly to the RF bandwidth while the limited bandwidth of the employed optical transmitter and receiver does. The results suggest that the transmission fluctuation is less than 5 dB.

### 3. Experimental system of 8 Gbps mm-wave beam steered RoF link based on the AWG-loop

The reversely-modulated DE-MZM mm-wave RoF link based on the integrated AWG-loop is schematically shown in Fig. 2. The 12.8 dBm wavelength-tunable optical carrier passes to a 10 GHz DE-MZM via a polarization

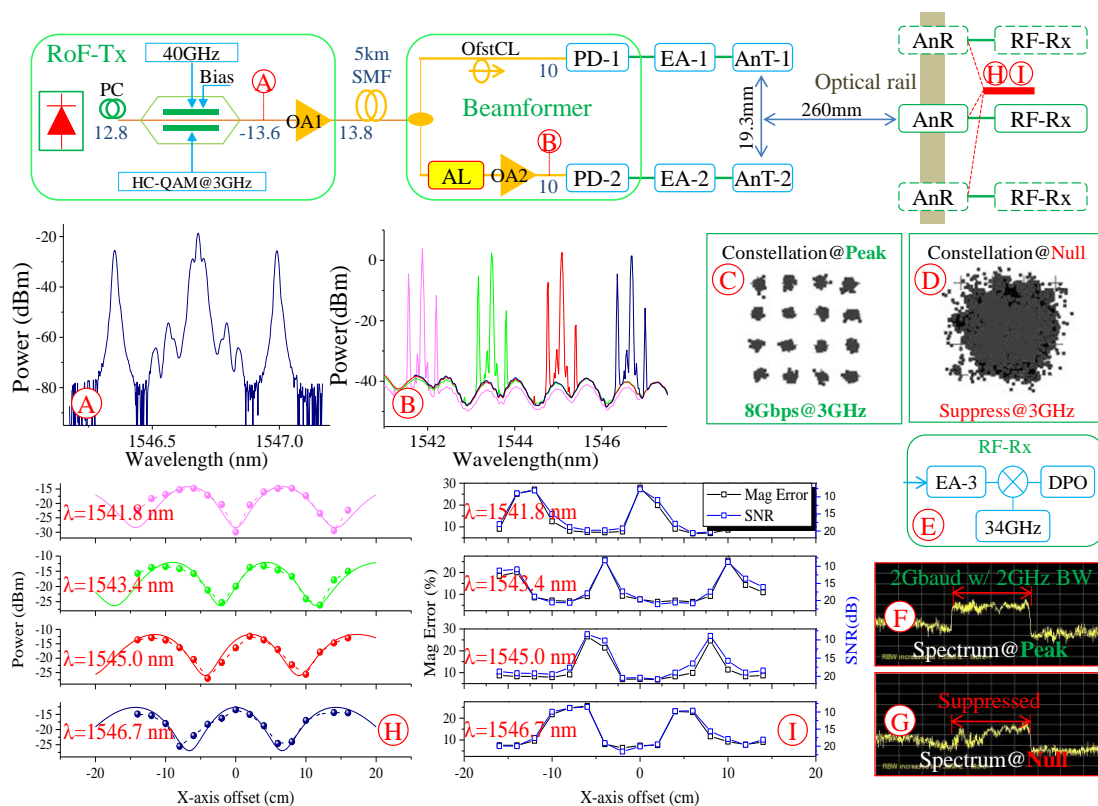


Fig. 2. Experimental setup and results of 40 GHz RoF link with optical radio beam steering based on integrated AWG-loop

controller. A 40 GHz clock signal is applied to the upper arm, and an 8 Gbps HC QAM-16 signal (2 Gbaud with 2 GHz bandwidth, raised cosine shaping,  $\beta=0.01$ , spectrum shown in Fig. 2(F)) at 3 GHz is applied to the lower arm. Here we use a cheap low-bandwidth DE-MZM as the HC QAM-16 signal is modulated in the low frequency range ( $<4.5$  GHz). The limited-bandwidth induced power fading just decreases the 40 GHz LO power rather than the HC QAM-16 signal quality. The MZM is biased at its power null point (E-field linear point) to allow high modulation efficiency. The data is modulated close to the center while the LO is modulated as sidebands with a so-called reversely-modulated manner. The spectrum of the modulated optical signal is shown in Fig. 2(A). Less than 10 dB carrier-to-sideband suppression is achieved for high modulation efficiency. After 5 km SMF, the optical signal is split into two paths. One directly connects to a photodiode (PD-1) with a bulk tunable offset compensation line (OfstCL). The other passes through the AWG-loop coupled by two cleaved SMFs. The converted signals are then amplified by two 40 GHz band amplifiers (EA-1 and EA-2) to transmit the HC QAM-16 signal wirelessly via two identical 40 GHz aperture antennas (AnT-1/-2). A 40 GHz aperture antenna (AnR) for receiving the wireless signal is moved along an optical rail. A RF receiver (RF-Rx) comprises an electrical down-converter (shown in Fig. 2(E)) and a real time 50 GSaps oscilloscope (DPO) for signal demodulation and analysis. Geometric parameters for the antenna locations can be found in Fig. 2. Four spatial channels can be steered by tuning the wavelength of the optical carrier. The spectra of the tuned wavelengths at 1541.8, 1543.4, 1545.0, 1546.6 nm are depicted in Fig. 2(B). Their intentional asymmetric profiles form single sideband modulation which can avoid frequency fading effects.

#### 4. Experimental results and discussion

As shown in Fig. 2(H), the measured power (dot) along x-axis and its simulated counterpart (line) are depicted one by one for all four wavelengths (delays). We can clearly see that the experimental results match well with the simulated ones in terms of peak/null locations and their periodicities. In the real environment, the difference between two results may be introduced by the inevitable mm-wave reflection. Wavelength tuning results in delay tuning and further controls radio beam directions. As the wavelength increases from 1541.8 nm to 1546.6 nm, the delays decrease from 12 ps to 0 ps as shown in Fig. 1(b) which results in the beam peaks moving from the left side to the right side. For phased array antennas, it is well known that the side lobes can be suppressed if the element antenna distance  $d$  is smaller than one half of the mm-wave wavelength ( $\lambda_{mm}$ ). In our experiment, due to the bulk aperture antennas, the distance  $d$  is 1.93 cm, which is much larger than one half of  $\lambda_{mm}$  (0.39 cm), thus the side lobes exist, resulting in more than one peak in the beam profiles as shown in Fig. 2(H) and (I). They can be easily avoided by using patch antennas. The power suppression ratios for all delays are more than 14 dB. This means a 14 dB channel isolation which is good enough for independent spatial channels. It can be further improved with a good power balance between PD-1/-2 or with a larger antenna array. The simulation well predicts such unbalance as shown in Fig. 2(H). The signal-to-noise ratio (SNR) shown in Fig. 2 (I) is measured based on the received power of wireless signals, which exhibits a good matching with the measured power in Fig. 2(H). The error vector magnitude (EVM) of the 8 Gbps HC QAM-16 signal is measured in Fig. 2(I). The EVM curves show a very good matching with the SNR curves as we expected. Thus, it is evident that beam steering allocates the power peak to a specified location. The resulting SNR enhancement allows a good signal performance (in terms of EVM). Two representative constellations at a peak and a null are shown in Fig. 2(C) and (D). At the peak, the EVM is 7% and the constellations are well converged as shown in Fig. 2(C). Its RF spectrum is shown in Fig. 2(F). At the null, the received power is reduced by 14 dB. Such low received power cannot even allow the demodulation of HC QAM-16 signal. Its RF spectrum shown in Fig. 2(G) indicates an evident power suppression.

#### 5. Conclusion

In this paper, we demonstrated a beam-steered 40 GHz fiber mm-wave link to wirelessly deliver 8 Gb/s HC QAM-16 signal to four spatial channels/beams. The simplified remotely-controlled photonic integrated OTDL, reversely-modulated single sideband modulation with high modulation efficiency, and Nyquist subcarrier modulation with high spectral efficiency guarantee its high energy-spatial-spectral efficiency. We believe that the proposed system provides a novel system concept for 5G back-/front-haul.

**Acknowledgement** We would like to thank Drs. E. Smalbrugge and Dr. X. Leijtens from TU/e, Dr. F. M. Soares from HHI for necessary measurement support. We thank the financial support from ERC FP-7 advanced grant BROWSE (291632), and ERC FP-7 project grant PARADIGM (257210).

#### 6. References

- [1] W. Roh et al., IEEE Comm. Mag. **52**(2), 106-113 (2014)
- [2] Z. Cao et al., IEEE PTL **26**(6), 575-578 (2014)
- [3] Z. Cao et al., OSA Opt. Lett. **40**(17), 3930-3933 (2015)
- [4] F. M. Soares et al., OATA/IPR 2004, p. IFB2 (2004).
- [5] M. A. Piqueras et al., IEEE TMTT **54**(2), 887-899 (2006).
- [6] T. P. McKenna, et al., IEEE PTL **26**(14) 1407-1410 (2014)